Article

Simulations and Experimental Investigations on the Acoustic Characterization of Centrifugal Pumps of Different Specific Speed †

Christian Lehr *,‡, Andreas Linkamp ‡, Daniel Aurich ‡ and Andreas Brümmer ‡

Chair of Fluidics, TU Dortmund University, 44227 Dortmund, Germany
* Correspondence: christian.lehr@tu-dortmund.de
† This paper is an extended version of our paper in Proceedings of the 13th European Turbomachinery Conference on Fluid Dynamics & Thermodynamics ETC13, Lausanne, Switzerland, 8–12 April 2019. Paper No. 150.
‡ These authors contributed equally to this work.

Abstract: Subject of discussion are simulations and experimental investigations on the acoustic characterization of three single stage centrifugal pumps of different specific speed. In operation, these pump-types generate pressure pulsation at blade passing frequency, primarily due to rotor-volute-interaction. In order to determine the acoustic excitation it is necessary to know about the pumps' acoustic transmission parameters. In this paper, a one-dimensional numerical model for transient time-domain simulation is presented, which takes into account the pump geometry as well as the volutes' structural behaviour by means of the local effective speed of sound. Numerical results for the transmission characteristics of the three different pumps are shown in terms of scattering matrices and evaluated against parameters calculated from measurement results. The experimental analyses are carried out using dynamic pressure sensors in both the suction and the discharge pipe. Assuming solely plane wave propagation, the complex acoustic field on each side is evaluated independently. The so called "two source" method is then used to determine the transmission parameters of the pumps in standstill for a range of frequencies experimentally. Subsequently, the acoustic excitation at varying rotational speed is evaluated by means of measurements at the pumps in operation and presented as monopole and dipole source types for cavitation-free conditions.

Keywords: centrifugal pump; pressure pulsation; acoustic transmission; scattering parameters; one-dimensional model

1. Introduction

The pressure and velocity pulsations in centrifugal pumps can be attributed to a non-uniform pressure and velocity distribution along the impeller outlet and an amplification of these conditions caused by an interaction with the volute tongue or rather the surrounding guide vanes [1,2]. The source strength significantly depends on the pumps geometry [3,4] and operation parameters as rotational speed and operation point [5,6]. The occurring pressure amplitudes in connected pipe systems due to this source of sound are influenced by the acoustic impedance of the piping [7] just as the pumps transmission behaviour itself. In case of resonances, this finally leads to increased vibrations and noise emission.

In order to determine the acoustic excitation caused by centrifugal pumps from dynamic pressure measurements, the transmission behaviour of the pump must be known. Provided that wave propagation is linear and plane, a centrifugal pumps transmission characteristic can be described as an acoustic four-pole and therefore by means of four parameters. Measurement of four-pole matrices

requires a complex experimental setup with additional acoustic sources. In order to reduce the experimental effort and thus provide a practically feasible method for the determination of source parameters, the pumps' transmission properties can be modelled. One approach in this context is the approximation of transmission parameters by lumped parameter models in the frequency domain analogue to electric networks [8,9]. Interactions of pump transmission, source and piping system can be calculated analytically in the frequency domain. One major disadvantage in this context is the missing connectivity of these models to time-dependent processes such as opening valves in a connected piping or cavitation phenomenons.

A second approach and at once the one described in this paper is based on numerical time-domain simulations. If the fundamental process of pulsation generation should not be investigated but rather the quantitative occuring pressure pulsations a one-dimensional numerical model is sufficient. As described in [10], the acoustics of an active pump can be simulated in arbitrary pipe systems by means of a passive pump model which is extended by prescribed point sources of monopole and dipole type. Based on this previous work, a simple one-dimensional model for single stage centrifugal pumps is described hereinafter. It preserves the determination of transmission behaviour taking the pumps' geometries as well as the influence of structure into account. Simulation results of the transmission parameters for three centrifugal pumps of different specific speed are presented and evaluated by means of measurement results. Source parameters based on dynamic pressure measurements of these pumps in operation are calculated for simulated and measured pump transmission parameters.

2. Experimental Setup and Determination of Parameters

In order to obtain the acoustic pump parameters experimentally, a setup as shown in Figure 1 was used. The pump under investigation was $P1$. On each side of the pump, up-(u) and downstream (d), four piezoelectric pressure transducers are flush mounted to the inner pipe wall to detect the pulsations at four non-equidistant positions. For a regular operation of $P1$, the primary pipe system is provided while the operation point can be adjusted by means of a control valve. The second pump $P2$ within the secondary pipe system is solely used as an external source of sound in order to determine the scattering parameters of the pump under investigation $P1$. The approach is explained later on.
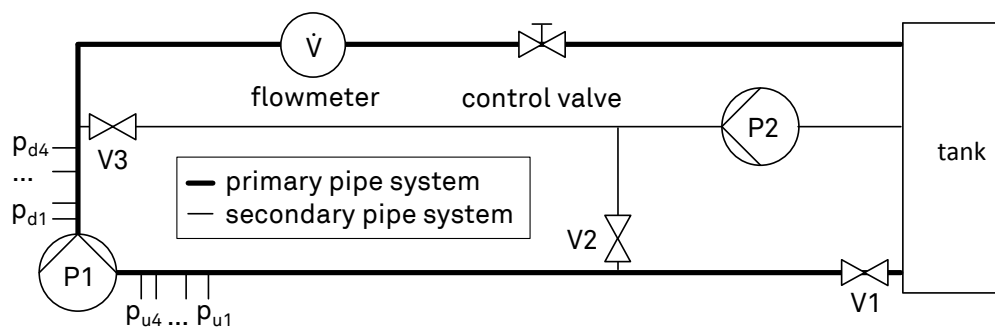

Figure 1. Experimental setup for the determination of acoustic pump parameters.

In Figure 2 a characteristic example for measured pressure amplitudes generated by the centrifugal pump $P1$ in operation at blade passing frequency including an envelope based on the measurements is given. The pressure amplitude is variable in space due to reflections in the connected piping system. As regards the comparison of amplitudes up- and downstream, it becomes clear that the pumps transmission behaviour is characterized by strong reflections. Consequently, the transmission parameters of the pump must be known to distinguish between system response and initial source.
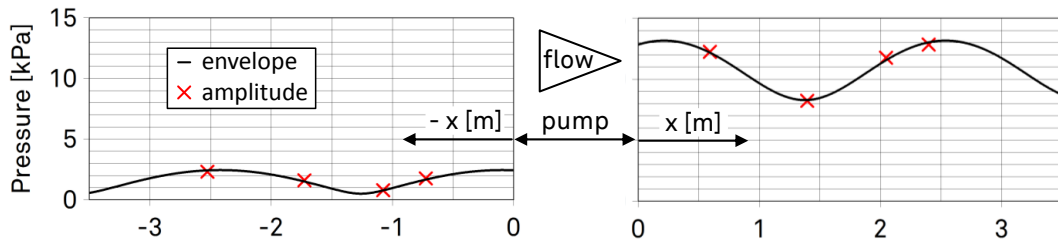
Figure 2. Measured and least-square fitted envelope of the pressure amplitudes $\hat{p}(x_n)$ upstream and downstream of the pump as a function of location ($P1 : n_s = 25 \frac{1}{min}$ in nominal operation point at $f_{BP} = 290$ Hz).

The experimental determination of acoustic pump parameters is based on transient pressure measurement in both the up- and downstream piping of the pump. Each dynamic pressure signal $p_{ex}(t, x_n)$ measured at the different sensor positions x_n was Fourier-transformed into the frequency domain. All considerations in this work refer to the pulsation generation and transmission at blade passing frequency f_{BP} which can be calculated as a function of number of blades z and rotational speed n_r to $f_{BP} = z \cdot n_r \cdot \frac{1}{60s}$. Therefore, complex amplitudes $\underline{\hat{p}}_{ex}$ were at blade passing frequency f_{BP}. The following shall give a short description on how the sound fields on both pump sides are evaluated.

Generally, a complex pressure amplitude $\underline{\hat{p}}$ at location x_n can be regarded as a superposition of a forward and a backward running acoustic wave $\underline{\hat{f}}$ and $\underline{\hat{g}}$, often referred to as Riemann invariants

$$\underline{\hat{p}}(x_n) = \underline{\hat{f}} \cdot e^{-ikx_n} + \underline{\hat{g}} \cdot e^{ikx_n}. \tag{1}$$

These Riemann invariants are assumed as constant (invariant) for each operating point in each piping section with constant cross-section. The wave number k is defined as a function of frequency f and the effective speed of sound a_{eff} in the piping (later assumed to 1350 $\frac{m}{s}$):

$$k = \frac{2\pi f}{a_{eff}}. \tag{2}$$

In order to evaluate the up- and downstream sound fields, $\underline{\hat{f}}$ and $\underline{\hat{g}}$ have to be determined for both sides separately. Since Equation (1) comprises two unknowns, the evaluation for four pressure signals leads to an overdetermined system, which is solved in a least square manner in order to receive the best fit for $\underline{\hat{f}}$ and $\underline{\hat{g}}$. For a more detailed description of the method refer to [11]. In order to quantify the residuum of the solution found, a relative error E_{rel} is determined by:

$$E_{rel} = \sqrt{\frac{\sum_{n=1}^{4} |\underline{\hat{p}}_{ex}(x_n) - \underline{\hat{p}}(x_n)|^2}{4 \cdot \hat{p}_{max}^2}} \cdot 100\% \quad \text{with} \quad \hat{p}_{max} = |\underline{\hat{f}}| + |\underline{\hat{g}}|. \tag{3}$$

Since $\underline{\hat{f}}$ and $\underline{\hat{g}}$ are known, the active pump can be described by means of a four-pole via a scattering matrix which contains the transmission parameters $(\underline{\hat{t}}_{ud}, \underline{\hat{r}}_d, \underline{\hat{r}}_u, \underline{\hat{t}}_{du})$ and an additional term representing the complex invariant source amplitudes $\underline{\hat{f}}_s$ and $\underline{\hat{g}}_s$

$$\begin{pmatrix} \underline{\hat{f}}_d \\ \underline{\hat{g}}_u \end{pmatrix} = \begin{bmatrix} \underline{\hat{t}}_{ud} & \underline{\hat{r}}_d \\ \underline{\hat{r}}_u & \underline{\hat{t}}_{du} \end{bmatrix} \begin{pmatrix} \underline{\hat{f}}_u \\ \underline{\hat{g}}_d \end{pmatrix} + \begin{pmatrix} \underline{\hat{f}}_s + \underline{\hat{r}}_d \underline{\hat{g}}_s \\ \underline{\hat{t}}_{du} \underline{\hat{g}}_s \end{pmatrix}. \tag{4}$$

Figure 3 illustrates the parameters of Equation (4) in a schematic pump surrounding. The source is located at the downstream side of the pump corresponding to the assumed origin of pulsation generation in centrifugal pumps described above. The scattering parameters $\underline{\hat{r}}_u$ and $\underline{\hat{r}}_d$ quantify the

acoustic reflection properties of the pump. Scattering parameters $\hat{\underline{t}}_{ud}$ and $\hat{\underline{t}}_{du}$ define the part of sound that is transferred from one side of the pump to the other.
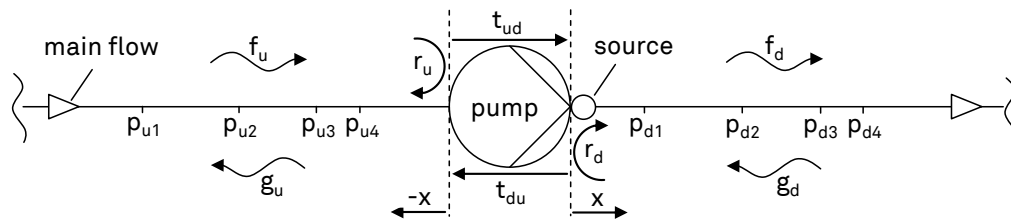

Figure 3. Four-pole representation of the pump via scattering parameters.

For the experimental determination of the pumps scattering parameters, a second pump $P2$ is used as an external source of sound while pump $P1$ stands still. The used approach is called a "two-source" method and is described in [12]. As shown in Figure 1, $P2$ is located in a secondary pipe system. By means of valves $V2$ and $V3$, the direction from where the sound is arriving $P1$ can be varied. In order to derive the four parameters analytically, two linear independent tuples of invariants $\hat{\underline{f}}$ and $\hat{\underline{g}}$ are required. To improve the validity of results, an over-determination of the four pole data, described by [13], is created by using the following expression with three linear independent states of sound (superscripts a, b, and c):

$$
\begin{bmatrix} \hat{\underline{t}}_{ud} & \hat{\underline{r}}_d \\ \hat{\underline{r}}_u & \hat{\underline{t}}_{du} \end{bmatrix} = \begin{pmatrix} \hat{\underline{f}}_d^a & \hat{\underline{f}}_d^b & \hat{\underline{f}}_d^c \\ \hat{\underline{g}}_u^a & \hat{\underline{g}}_u^b & \hat{\underline{g}}_u^c \end{pmatrix} \begin{pmatrix} \hat{\underline{f}}_u^a & \hat{\underline{f}}_u^b & \hat{\underline{f}}_u^c \\ \hat{\underline{g}}_d^a & \hat{\underline{g}}_d^b & \hat{\underline{g}}_d^c \end{pmatrix}^{-1}.
\tag{5}
$$

The associated valve settings for each state of sound (a,b,c) are as specified in Table 1. By keeping the valves $V1$ and the control valve closed, it was ensured that no volume flow through pump $P1$ was generated and thus no relevant additional sources of sound within the pump occurred.

Table 1. Valve settings for the states of sound a,b, and c.

State of Sound	V1	V2	V3	Control Valve
a	closed	open	closed	closed
b	closed	closed	open	closed
c	closed	open	open	closed

With the knowledge of the pumps transmission parameters, the excitation source parameters can be estimated. As Equation (4) is just one form of representation, the source parameters can also be calculated as monopole $\hat{\underline{p}}_s$ and dipole $\hat{\underline{c}}_s$ types if the following expression is used:

$$
\hat{\underline{p}}_s = \frac{1}{2}(\hat{\underline{f}}_s + \hat{\underline{g}}_s)
\tag{6}
$$

$$
\hat{\underline{c}}_s = \frac{1}{2}(\hat{\underline{f}}_s - \hat{\underline{g}}_s)\frac{1}{\rho_f a_{eff,d}}.
\tag{7}
$$

Within this equation ρ_f is the mean density of the fluid and $a_{eff,d}$ the effective speed of sound in the source region. The monopole is a source of mass and thus generating pressure pulsations which are -related to the source's point of origin- in phase to each other in up- and downstream direction. The dipole in turn is defined as a source of momentum and therefore a source of velocity fluctuations in the fluid which leads to pressure waves reversely phased in both directions. The superimposed results $\hat{\underline{f}}_s$ and $\hat{\underline{g}}_s$ of both source types are pulsations which are defined by magnitude and phase relationship between monopole and dipole.

Int. J. Turbomach. Propuls. Power **2019**, *4*, 16

5 of 12

Pumps under investigation were three radial single stage centrifugal pumps with six vanes impeller which were associated to one product line but were not geometrically similar. All pumps had a nominal pipe diameters of DN80 at suction and DN65 at discharge side. The listed best point values discharge head H_N and volume flow $\dot{V}_N$ in Table 2 are referred to a rotational speed of $n_r = 2900 \frac{1}{min}$. The specific speed n_s is determined by means of the following definition:

$$n_s = n_r \cdot \frac{\dot{V}_N^{\frac{1}{2}}}{H_N^{\frac{3}{4}}} \quad \text{with} \quad \dot{V}_N \text{ in } \left[\frac{m^3}{s}\right], \ H_N \text{ in } [m], \ n_r \text{ in } \left[\frac{1}{min}\right]. \tag{8}$$

All investigated measurement data regarding this work were limited to cavitation free operation for the pumps under test. In order to ensure this condition, the $NPSH_a$ parameter within the experimental setup, which quantifies the distance between the total pressure at the pumps upstream port $p_{t,u}$ and the vapour pressure p_v

$$NPSH_a = \frac{p_{t,u} - p_v}{\rho \cdot g}, \tag{9}$$

was prescribed at $NPSH_a = 45\,\text{m}$. As a previous work of the authors [14] has shown, there is no influence of cavitation onto the pressure pulsations for the investigated pump type at this $NPSH_a$ value.

Table 2. Specifications of the investigated pumps.

n_s [1/min]	Outer Impeller Diameter [mm]	min. Impeller − Volute Distance [mm]	H_N [m]	$\dot{V}_N$ [m³/h]
25	219	8.1	62	124
37	174	9.6	34	115
52	141	8.3	21	114

3. One-Dimensional Model

The applied numerical scheme is based on the non-linear one-dimensional conservation equations for mass and momentum in characteristic form (MOC):

$$\frac{dp}{dt} + \rho a \frac{dc}{dt} = 0 \quad \text{along} \quad \frac{dx}{dt} = c + a \tag{10}$$

$$\frac{dp}{dt} - \rho a \frac{dc}{dt} = 0 \quad \text{along} \quad \frac{dx}{dt} = c - a \tag{11}$$

For the solution of Equations (10) and (11) an in-house solver called FLOAT was used. Isothermal and inviscid flow was assumed. The numerical solution was carried out by using a finite-difference scheme with first order upwind discretization. For the temporal discretization, an explicit Euler scheme was applied. Therefore the flow variables pressure p and velocity c at grid point i for the next time step $n + 1$ can be calculated by the following expressions:

$$p_i^{(n+1)} = \frac{1}{2} \left(\rho_i^n a_i^n \left(c_A - c_B\right) + \left(p_A + p_B\right) \right) \tag{12}$$

$$c_i^{(n+1)} = \frac{1}{2} \left(\frac{1}{\rho_i^n a_i^n} \left(p_A - p_B\right) + \left(c_A + c_B\right) \right). \tag{13}$$

As shown in Figure 4 the superscripts A and B relate to the base points of the two sound characteristics of the up- $(c - a)$ and downstream $(c + a)$ running wave at timestep n. A comprehensive explanation of the method used is described in the authors' previous work [15].
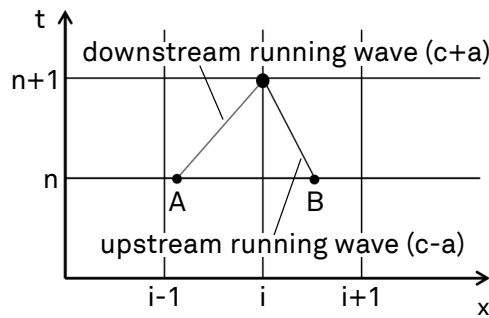
Figure 4. Time-space-grid with indicated base points A/B for positive direction of flow.

The following paragraph elucidates the model approach of the pumps' transmission behaviour which has geometrical and structural influences. As illustrated in Figure 5, the reduced pump model's geometry was divided into three parts named as upstream port (up), chamber (ch), and downstream port (dp). Every part was defined via the two geometric parameters length l and diameter d which are derived from the following conditions:

- the total fluid volume of the original pump $V_{f,o}$ and the model $V_{f,m}$ are equal and therefore $V_{f,o} = V_{f,m} = V_{up} + V_{ch} + V_{dp}$
- lengths (l_{up}, l_{dp}) and diameters (d_{up}, d_{dp}) of up- and downstream port (and thus volumes (V_{up}, V_{dp})) correspond to the pump ones and are directly derivable out of the pump's computer-aided design (CAD) model
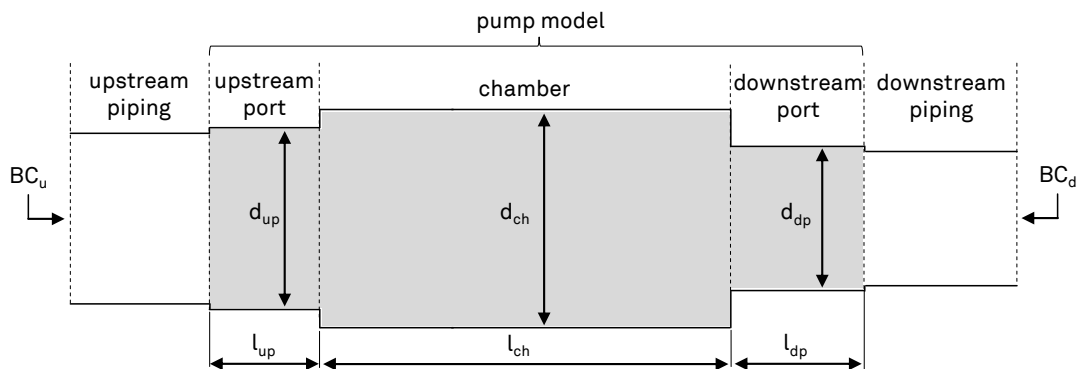- the mean acoustic length through the pump's. impeller and spiral defines l_{ch}

Figure 5. Geometric parameter of the reduced pump model.

The last mentioned mean acoustic length l_{ch} is calculated as the arithmetic mean value of the longest and shortest distance that sound waves travel through impeller and subsequent spiral $l_{ch} = \frac{l_{long} + l_{short}}{2}$. An illustration is shown in Figure 6 by means of the pumps CAD model. Finally, the last geometric parameter d_{ch} is derived by $d_{ch} = \sqrt{\frac{4V_{ch}}{\pi l_{ch}}}$.

Int. J. Turbomach. Propuls. Power **2019**, *4*, 16
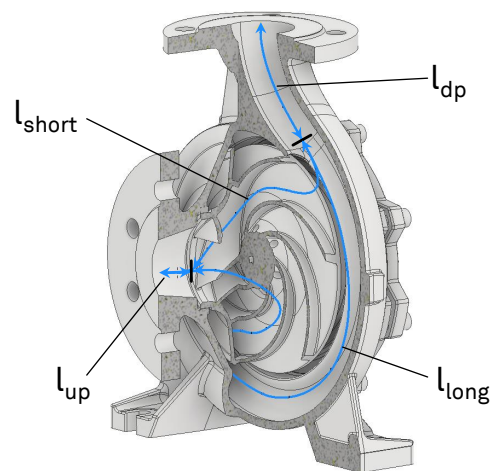
7 of 12

Figure 6. Illustration of the relevant acoustical lengths in a CAD model.

Previous experimental and numerical studies showed that a purely geometric based model as described above fits the pumps transmission behaviour only with air as working fluid. Measurements for the same configuration but water instead of air show significant stronger reflections and lower transmissions of sound that cannot be exclusively caused by the pump's geometry. The assumption that due to the significant lower compressibility of water, a compliance of the pump's structure reduces the effective speed of sound in the pump which leads to the varying transmission behaviour, follows. For example, Nicolet et al. [16] calculate the effective speed of sound within a scaled francis turbine by means of FEM simulations to develop a suitable one-dimensional hydroacoustic model.

The effective speed of sound a_{eff} in a fluid of volume V surrounded by a compliant body is a function of the speed of sound in the fluid a_f, the mean density ρ_f and a relative change of volume $\frac{\Delta V}{V}$ due to a pressure difference in the fluid Δp [17]:

$$a_{eff} = \frac{1}{\sqrt{\frac{1}{a_f{}^2} + \frac{\rho_f}{V}\frac{\Delta V}{\Delta p}}}. \tag{14}$$

Due to small changes of volume ΔV the deformation of the pump's housing is assumed to be linear elastic. Therefore the ratio $\frac{\Delta V}{\Delta p}$ is constant.

In order to take the change of structural compliance within the pump's housing into account the speed of sound inside the model is prescribed in sections (indices up, ch, and dp). As in [16], FEM simulations are necessary to derive $\frac{\Delta V}{\Delta p}$ and hence a_{eff}. However, in order to consider the structural impact for the investigated pumps, within this paper an alternative way is used. The effective speed of sound within the model's chamber $a_{eff,ch}$ is reduced iterativly until the transmission parameters fit the measured ones.

The effective speed of sound within the up- and downstream port $a_{eff,up}$ and $a_{eff,dp}$ are assumed to be equal to the effective speed of sound within the connected piping ($a_{eff,u}$ and $a_{eff,d}$). This value in turn is determined from the least square procedure. The best approximation for $\hat{f}$ and $\hat{g}$ is a function of the actual effective speed of sound within the measuring tubes. All applied model parameters for the pumps under test are summarized in the next section.

For the numerical determination of the model's transmission parameters analogous to Equation (5), two lineary independent states (a/b) are sufficient. The states were created by using either a prescribed harmonic velocity at boundary condition BC_u while BC_d is reflection-free (a) or vice versa (b).

Int. J. Turbomach. Propuls. Power **2019**, *4*, 16

8 of 12

4. Results

Table 3 below contains the derived geometric model parameters as well as the effective speeds of sound for every investigated pump. As described above, the geometric values of the up- and downstream ports were directly determined by the pumps' CAD model. The models' chamber geometry was a conclusion of CAD data and acoustic length.

Furthermore, it becomes apparent that the effective speed of sound $a_{eff,ch}$, to model the pumps' structural compliance due to pressure pulsations, was small compared to the pure fluid $(a_f = 1477 \frac{m}{s}$ [18]) and increases significantly with the value of specific speed n_s. It is suspected that this tendency is a consequence of the respective housing designs. To name an example of reverse tendency, in case of an axial centrifugal pump ($n_s > 170 \frac{1}{min}$) the volute was cylindrically shaped, comparable to a simple tube, and therefore less compliant. In conclusion, that means the higher the specific speed the lower the impact of structural compliance on the transmission behaviour of the investigated pump types.

Table 3. Geometric and structural influenced model parameters of the investigated pumps.

	Geometric Parameters [mm]						Speeds of Sound a_{eff} [$\frac{m}{s}$]		
n_s [1/min]	d_{up}	l_{up}	d_{ch}	l_{ch}	d_{dp}	l_{dp}	$a_{eff,up}$	$a_{eff,ch}$	$a_{eff,dp}$
25	88	45	95	509	68	114	1350	650	1350
37	88	45	95	408	65	78	1350	850	1350
52	89	49	103	333	72	75	1350	1025	1350

As per description, the effective speeds of sound $a_{eff,up}$ and $a_{eff,dp}$ within the model's up- and downstream port are prescribed to be equal to the speed of sound within the measuring tubes up- and downstream. For a value of $a_{eff,u} = a_{eff,d} = 1350 \frac{m}{s}$ in Equation (2) for use in Equation (1) the approximation of $\hat{f}$ and $\hat{g}$ fits at best for a major part of the evaluated pressure measurements. The standard deviation of the least square procedures' relative error E_{rel} (Equation (3)) over all solutions applied in this work based on measurements are listed in Table 4.

Table 4. Standard deviation of the least square procedures' (LSF) relative error E_{rel} for $a_{eff,u} = a_{eff,d} = 1350 \frac{m}{s}$.

Parameter	Value	Explanation
k	318	total number of LSF performed
$\overline{E_{rel}} = \frac{1}{k}\sum_{i=1}^{k} E_{err}$	2.2%	mean relative error over all LSF
σ	3.5%	68.27% of all E_{rel} are smaller
$2 \cdot \sigma$	6.9%	95.45% of all E_{rel} are smaller
$3 \cdot \sigma$	10.4%	99.73% of all E_{rel} are smaller

Based on the data in Table 3, the numerical transmission parameters were obtained and evaluated against measurement results. In this context, magnitudes of experimental and simulated scattering parameters are shown in Figure 7 as a function of frequency. The model parameters (see Table 3) used to calculate the scattering parameters are assumed to be frequency independent.
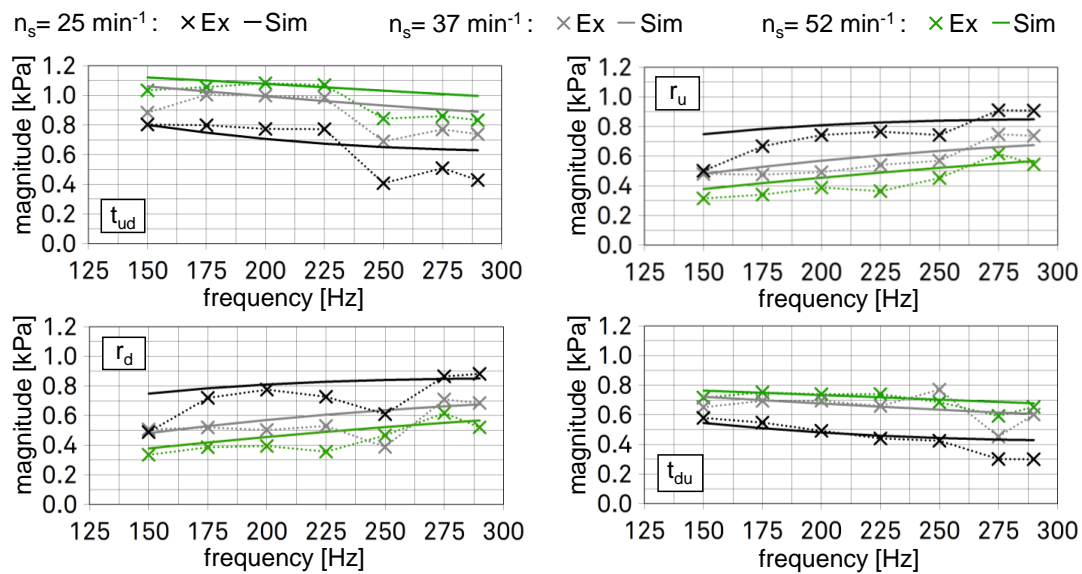
Figure 7. Comparison of experimental (Ex) and simulated (Sim) magnitudes of the transmission parameters $\hat{\underline{r}}_u$, $\hat{\underline{t}}_{ud}$, $\hat{\underline{t}}_{du}$ and $\hat{\underline{r}}_d$ as a function of frequency for all investigated specific speeds.

In general, a good agreement of simulated and experimental results can be obtained. Furthermore, it becomes apparent that for every parameter a systematic arrangement of curves due to an impact of specific speed or respectively the type of pump exists. While the magnitudes of both reflection parameters are the greatest for low specific speed the magnitudes of transmission are of reverse tendency. This trend can be recognized for both experiments and simulations and is therefore an indicator for a good model accuracy. The mean value of differences between simulated and experimental derived magnitudes over all frequencies and for all pump types was 9%. Greatest deviations were located at 250 Hz for the parameters $\hat{\underline{t}}_{ud}$ and $\hat{\underline{r}}_d$. Especially, for $\hat{\underline{t}}_{ud}$ the outliers of the measured parameters for all tested pump types at this frequency differ from the indicated trend. One reason could be that the prescribed effective speed of sound within the models' chamber $a_{eff,ch}$ is not a function of frequency and therefore possible eigenvalues of the pumps' or surrounding structure are influencing the transmission characteristics but are not taken into account. Aside from this the general agreement of simulated and measured transmission parameters for all investigated pump types is good.

The transmission parameters' phases are not shown but are briefly commented on in the following. The agreement between modelled and experimental determined phases over all frequencies was continuously good and in total better than the correspondence of magnitudes. Maximum deviations between measurement and simulation are up to 32° for a few single frequencies. The mean value of phase deviations for all transmission parameters was approximately 8°.

Overall, it can be summarized that a reduced one-dimensional model, as presented above, gives a good approximation of a centrifugal pumps transmission characteristic.

Once the scattering matrix parameters are known, the source terms can be obtained according to Equation (4). Therefore, measurements are performed while $P1$ is operating within the primary pipe system (see Figure 1) in adjusted operation points. The resulting dynamic pressure signals are again used to evaluate the Riemann invariants $\hat{f}$ and $\hat{\underline{g}}$ at blade passing frequency. In Figure 8 the source parameters' magnitudes and phase differences are shown in the form of monopole and dipole types p_s and $c_s(\rho_f a_{eff,d})$ for all investigated pumps at nominal operation points as a function of frequency.
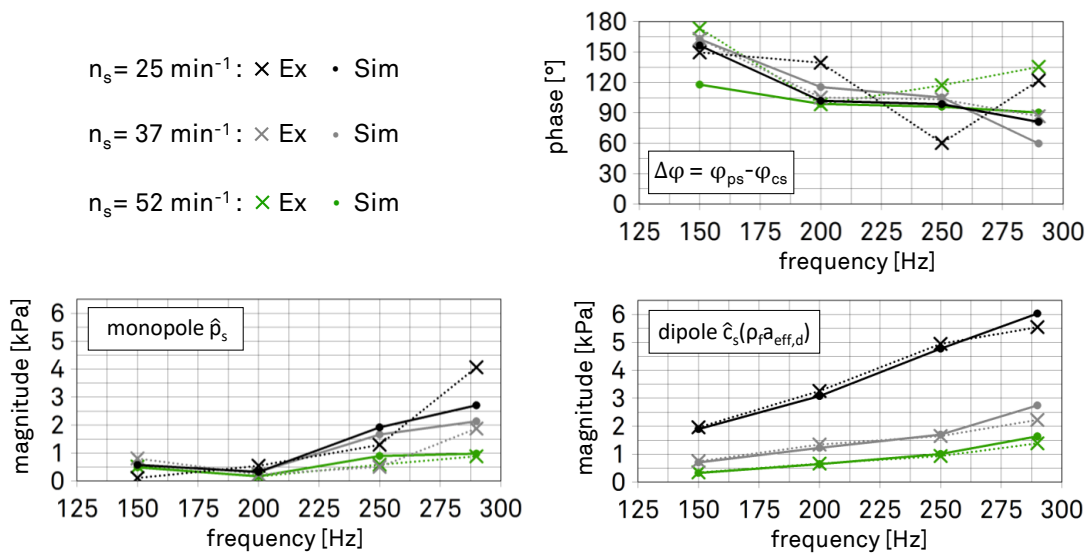
Int. J. Turbomach. Propuls. Power **2019**, *4*, 16

10 of 12

Figure 8. Experimental determined magnitudes and phase differences of monopole p_s and dipole $c_s(\rho_f a_{eff,d})$ source as a function of frequency using the experimental (Ex) or numerical (Sim) obtained transmission parameters for nominal operation points.

As the source region is assumed to be located in the downstream port, the effective speed of sound is set as $a_{eff,d} = 1350 \frac{m}{s}$. The mean density of the fluid is assumed as constant to ρ_f (20 °C) $= 998 \frac{kg}{m^3}$ [18]. The results are based on either experimental (Ex) or numerical (Sim) obtained transmission parameters. The dipole's magnitude is represented as $\hat{c}_s(\rho_f a_{eff,d})$ in pressure dimension to enable a better comparison. The general agreement between experimental and numerical based parameters are satisfactory in both phases and magnitudes. Especially, the dipole magnitudes show minor deviations. In comparison, phases ($\Delta\varphi$) and monopole magnitudes differ slightly more. In an overall assessment, it can be noted that the magnitudes of both source types, experimentally and numerically based, increase with higher frequencies. In [2] pressure magnitudes were nondimensionalized by $\frac{2\hat{p}}{\rho_f u_2^2}$. This indicated squared dependence on the impeller circumferential speed u_2 applies in particular to the dipole magnitudes. Furthermore, it can be constituted that -regarding to one frequency- monopole and dipole magnitudes increase with lower specific speed. Referring to experimental and numerical based parameters, the phase differences $\Delta\varphi$ for all pump types are basically decreasing from 150 to 290 Hz. With a few exceptions, values for 150 Hz were localized among 150° and 180° and for a frequency of 290 Hz between 60° and 90°. In order to interpret the phase relationship, it was necessary to define a zero phase angle which is considered as follows. If the phase angle between monopole and dipole is zero degree the superposition of both source types is maximally constructive in downstream and maximal destructive in upstream direction. In relation to the progression of phase values in Figure 8 follows that the superposition changes from rather destructive (150° < $\Delta\varphi$ < 180°) to neutral in upstream and reversed ordered in downstream direction.

5. Conclusions

The presented study describes a reduced model of the centrifugal pumps' transmission characteristics which is suitable for three pumps of different specific speed. The influencing geometric parameters are derived by the pumps' CAD model and a mean acoustic length through the pump. Due to the low compressibility of water, the compliance of structure influences the effective speed of sound in the pump. This effect is taken into account by an iteratively determined effective speed of sound as a model parameter for every pump type in particular. A comparison of numerically and experimentally determined scattering parameters confirms a good approximation of the model.

In addition, the model's quality is shown by the general good agreement of source parameters obtained by means of experimental or numerical based transmission parameters.

In further investigations, simulations of the pumps' structural behaviour will be carried out in order to confirm the effective speed of sound values, which are determined iteratively in this work. Apart from this, the effect of cavitation on the active and passive acoustic behaviour of centrifugal pumps will be investigated in order to enable the simulation over a wider operational range.

Author Contributions: writing—original draft preparation and visualization C.L.; software and writing—review and editing A.L.; supervision, funding acquisition, writing—review and editing A.B.; investigation, methodology and formal analysis C.L., A.L. and D.A.

Conflicts of Interest: The authors declare no conflict of interest. The funders had no role in the design of the study; in the collection, analyses, or interpretation of data; in the writing of the manuscript, or in the decision to publish the results.

Abbreviations

The following abbreviations are used in this manuscript:

parameters

a	$[\mathrm{m \cdot s^{-1}}]$	speed of sound
c	$[\mathrm{m \cdot s^{-1}}]$	sound particle velocity
d	$[\mathrm{m}]$	diameter
E_{rel}	$[\%]$	relative error
f	$[\mathrm{s^{-1}}]$	frequency
f	$[\mathrm{Pa}]$	invariant downstream running wave
g	$[\mathrm{Pa}]$	invariant upstream running wave
g	$[\mathrm{m \cdot s^{-2}}]$	gravitational constant
H	$[\mathrm{m}]$	discharge head
k	$[\mathrm{^\circ \cdot m^{-1}}]$	wave number
l	$[\mathrm{m}]$	length
n_r	$[\mathrm{min^{-1}}]$	rotational speed
n_s	$[\mathrm{min^{-1}}]$	specific speed
$NPSH$	$[\mathrm{m}]$	net positive suction head
p	$[\mathrm{Pa}]$	sound pressure
r	$[\text{-}]$	reflection coefficient
t	$[\text{-}]$	transmission coefficient
u	$[\mathrm{m \cdot s^{-1}}]$	circumferential speed
V	$[\mathrm{m^3}]$	volume
$\dot{V}$	$[\mathrm{m^3 \cdot s^{-1}}]$	volume flow
x	$[\mathrm{m}]$	axial coordinate
z	$[\text{-}]$	number of blades
ρ	$[\mathrm{kg \cdot m^{-3}}]$	mean density
φ	$[\mathrm{^\circ}]$	phase angle

indices

a	available
BP	blade passing
ch	chamber
d	downstream
dp	downstream port
eff	effective
ex	experimental

Int. J. Turbomach. Propuls. Power **2019**, *4*, 16

12 of 12

f	fluid
m	model
N	nominal operation
o	original
rel	relative
s	source
u	upstream
up	upstream port

References

1. Gülich, J. *Kreiselpumpen*, 4th ed.; Springer: Berlin/Heidelberg, Germany, 2013.
2. Brennen, C.E. *Hydrodynamics of Pumps*, 1st ed.; Cambridge University Press: Cambridge, UK, 2011.
3. Morgenroth, M.; Weaver, D. Sound Generation by a Pump at Blade Passing Frequency. *J. Turbomach.* **1998**, *120*, 736–743. [CrossRef]
4. Dong, R.; Chu, S.; Katz, J. Effect of Modification to Tongue and Impeller Geometry on Unsteady Flow, Pressure Fluctuations, and Noise in a Centrifugal Pump. *J. Turbomach.* **1997**, *506*, 506–515. [CrossRef]
5. Gülich, J.; Bolleter, U. Pressure Pulsations in Centrifugal Pumps. *J. Vib. Acoust.* **1992**, *114*, 272–279. [CrossRef]
6. Parrondo, J.; Pérez, J.; Fernández, J. The Effect of the Operation Point on the Pressure Fluctuations at the Blade-Passing Frequency in the Volute of a Centrifugal Pump. *J. Fluids Eng.* **2002**, *124*, 784–790. [CrossRef]
7. Keller, J.; Parrondo, J.; Barrio, R.; Fernández, J.; Blanco, E. Effects of the Pump-Circuit Acoustic Coupling on the Blade-Passing Frequency Perturbations. *Appl. Acoust.* **2013**, *76*, 150–156. [CrossRef]
8. Stirnemann, A.; Eberl, J.; Bolleter, U.; Pace, S. Experimental Determination of the Dynamic Transfer Matrix for a Pump. *J. Fluids Eng.* **1987**, *109*, 218–225. [CrossRef]
9. Bardeleben, M. Acoustic Characterization of a Centrifugal Pump Using a Two-Port Model. Ph.D. Thesis, McMaster University Hamilton, Hamilton, ON, Canada, 2005.
10. Linkamp, A.; Lehr, C.; Brümmer, A. Simplified one-dimensional model for transient time-domain simulation of centrifugal pumps. In Proceedings of the 24th International Congress on Sound & Vibration, London, UK, 23–27 July 2017; pp. 2377–2385.
11. Edge, K.; Johnston, D. The Secondary Source Method for the Measurement of Pump Pressure Ripple Characteristics. *J. Power Energy* **1990**, *204*, 33–40. [CrossRef]
12. Munjal, M.; Doige, A. Theory of a Two Source-Location Method for Direct Experimental Evaluation of the Four-Pole Parameters of an Aeroacoustic Element. *J. Sound Vib.* **1990**, *141*, 323–333. [CrossRef]
13. Allam, S.; Bodén, H.; Åbom, M. Over-Determination in Acoustic Two-Port Data Measurement. In Proceedings of the ICSV13-Vienna, The Thirteenth International Congress on Sound and Vibration, Vienna, Austria, 2–6 July 2006.
14. Lehr, C.; Linkamp, A.; Brümmer, A. Pulsationen an kavitierenden Kreiselpumpen bei Schaufelpassierfrequenz. In Proceedings of the Tagungsband DAGA, Kiel, Germany, 6–9 March 2017; p. 995.
15. Linkamp, A.; Deimel, C.; Brümmer, A.; Skoda, R. Non-reflecting coupling method for one-dimensional finite difference/finite volume schemes based on spectral error analysis. *Comput. Fluids* **2016**, *140*, 334–346. [CrossRef]
16. Nicolet, C.; Ruchonnet, N.; Avellan, F. One-Dimensional Modeling of Rotor Stator Interaction in Francis Pump-Turbine. In Proceedings of the 23rd IAHR Symposium on Hydraulic Machinery and Systems, Yokohama, Japan, 18–21 October 2006.
17. Horlacher, H.B.; Lüdecke, H.J. *Strömungsberechnung für Rohrsysteme*; Expert Verlag: Renningen, Germany, 2006.
18. Chen, C.T.A.; Millero, F. Precise thermodynamic properties for natural waters covering only the limnological range. *Limnol. Oceanogr.* **1986**, *31*, 657–662. [CrossRef]